Journal of Pharmacy

JOP
Journal of Pharmacy

Molecular Docking and Virtual Screening of *Tetracera macrophylla* Leaf Phytoconstituents Targeting Anticancer Therapy Development

Taslima Begum[1], Qamar Uddin Ahmed[1]*, Muhammad Akmal Hakim Ab Rahim[1], Syed Adnan Ali Shah[2], Mohd Salleh Rofiee[3], Mohd Hafiz Arzmi[4], ABM Helal Uddin[1], Zalikha Ibrahim[1], Kamal Rullah[1], Alfi Khatib[1]

[1]*Drug Discovery and Synthetic Chemistry Research Group, Department of Pharmaceutical Chemistry, Kulliyyah of Pharmacy, International Islamic University Malaysia, Kuantan 25200, Pahang, Malaysia.*

[2]*Faculty of Pharmacy, Atta-ur-Rahman Institute for Natural Products Discovery (AuRIns), Universiti Teknologi MARA, Cawangan Selangor Kampus Puncak Alam, 42300 Bandar Puncak Alam, Selangor, Malaysia.*

[3]*Integrative Pharmacogenomics Institute (iPROMISE), Universiti Teknologi MARA, Cawangan Selangor Kampus Puncak Alam, 42300 Bandar Puncak Alam, Selangor, Malaysia.*

[4]*Department of Fundamental Dental and Medical Sciences, Kulliyyah of Dentistry, International Islamic University Malaysia, 252 00 Kuantan, Pahang, Malaysia.*

Abstract

Introduction: Globally, the incidence of cancer is rising at an alarming rate. Among various types, breast cancer was reported as the most prevalent cancer in females in 2022, while melanoma represents an aggressive form of skin cancer characterized by the malignant transformation of melanocytes. To address the urgent need for new anticancer drugs, traditional medicinal plants offer significant potential. *Tetracera macrophylla* is widely used by the inhabitants across Asia and Africa to treat diverse ailments, making it a promising candidate for investigation. The objective of the current study was to prepare a polar compound-based methanol extract of *T. macrophylla* leaves and identify bioactive compounds with potential anticancer activity. **Methods**: A sequential extraction technique was employed to obtain the methanol extract enriched in polar compounds, which was subsequently analysed using Q-ToF LCMS for compound identification. The identified compounds were then screened *in silico* against two cancer-related proteins (PDB IDs: 3OG7 and 3ERT) to evaluate their potential against melanoma and breast cancer. Lead compound selection was further refined through physicochemical and pharmacokinetic parameter assessments. **Results**: The methanol extract (yield: 9.29%) revealed ten compounds, predominantly flavonoids. Molecular docking analysis demonstrated favourable binding energies and interactions of these compounds with the target proteins. Notably, eight compounds namely isovitexin, epigallocatechin 3-O-caffeate, 5,7,4'-trihydroxyflavanone 7-sulfate, 7,8,4'-trihydroxyflavanone, 4,2',3',4'-tetrahydroxychalcone, urolithin A-3-O-glucuronide, epifisetinidol-4alpha-ol, and epicatechin monogallate exhibited drug-likeness properties. **Conclusions**: Collectively, this study provides a strong foundation for further research into the development of novel anticancer drugs derived from *T. macrophylla* leaves, targeting breast cancer and melanoma.

Article history:

Received: 31 December 2025
Accepted: 22 April 2026
Published: 31 July 2026

Keywords:

Tetracera macrophyla
Q-ToF LCMS
Molecular docking
Breast cancer
Melanoma
Binding energy
Drug likeness

doi: 10.31436/jop.v6i2.489

*Corresponding author's email: quahmed@iium.edu.my

Introduction

Cancer is a broad term encompassing a large group of diseases that can affect virtually any part of the body. It is also referred to as a malignant tumour or neoplasm. A defining characteristic of cancer is the rapid formation of abnormal cells that proliferate beyond their normal boundaries, invading adjacent tissues and spreading to distant organs- a process known as metastasis. Widespread metastases are the leading cause of cancer-related mortality (World Health Organization, 2023). According to Globocan 2022, there were 19,976,499 new cancer cases and 9,743,832 cancer-related deaths worldwide in 2022. Among women, breast cancer accounted for the highest incidence, representing 23.8% of new cases (Bray *et al*., 2022). Estrogen receptors exist in two main forms, ERα and ERβ. Estrogens play a pivotal role in breast cancer progression, with ERα status serving as a key predictor of prognosis. In Asian countries, more than 60% of breast cancer cases are diagnosed as ERα-positive (Sahayarayan *et al*., 2021). Melanoma, an aggressive form of skin cancer, arises from the malignant transformation of melanocytes. One of the most frequently mutated oncogenes in melanoma is BRAF, which has become an important target for molecular therapy. The use of BRAF kinase inhibitors has demonstrated promising therapeutic outcomes (Castellani *et al*., 2023).

In addition to synthetic drugs, plant-based approaches hold significant promise for the development of new anticancer agents, particularly in addressing the rising incidence of cancer and the challenges of drug tolerance and adverse side effects. *Tetracera macrophylla* Hook.f. & Thomson is a woody climbing plant widely distributed across Asia and Africa (Fig. 1) and is traditionally used to relieve throat ailments and symptoms of tuberculosis (Mazlun *et al*., 2020). Previous scientific investigations have primarily focused on the antimicrobial properties of its leaves (Ladeska *et al*., 2023). However, to date, no studies have explored the anticancer potential of *T. macrophylla* extracts or their chemical constituents. Therefore, the objective of this study was to identify bioactive compounds present in the leaf extract of *T. macrophylla* that may serve as lead molecules for the development of novel anticancer drugs targeting melanoma and breast cancer.

Fig. 1: *T. macrophylla* leaves.

Materials and methods

Collection and preparation of plant sample

The collection and preparation of the final methanol extract from *T. macrophylla* leaves are presented in Fig. 2 (Ananda *et al*., 2025). This sequential extraction process enabled the isolation of a methanol extract enriched with polar compounds.

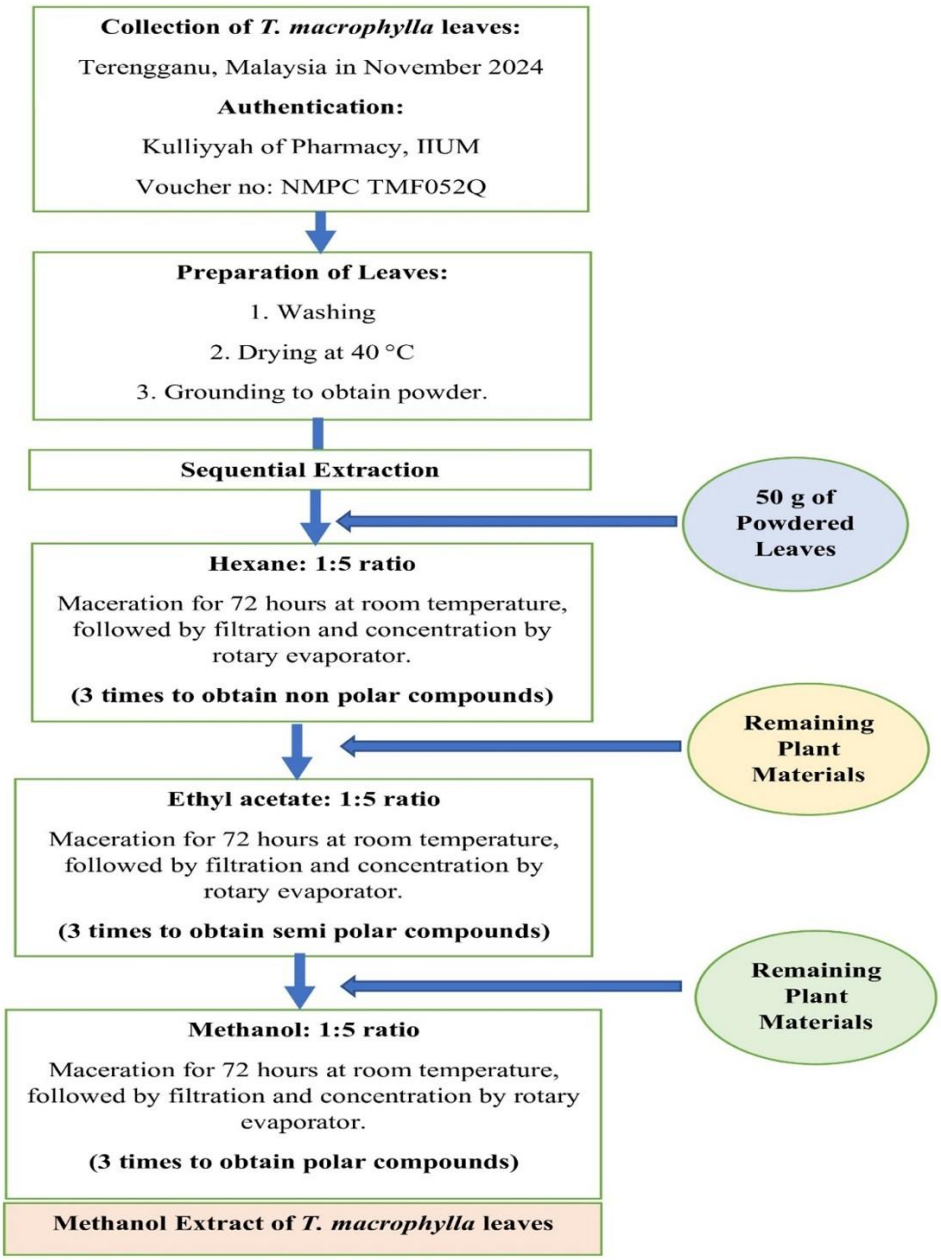

Fig. 2: Extraction procedure of methanol extract of *T. macrophylla* leaf**.**

Q-ToF LCMS analysis of phytochemicals in T. macrophylla leaf extract

The leaf extract of *T. macrophylla* was analyzed using an LC/MS-Q-ToF system comprising an Agilent 1200 liquid chromatography unit equipped with a binary pump, vacuum degasser, autosampler, and an Agilent 6520 quadrupole time-of-flight mass spectrometer with an electrospray ionization (ESI) source. Chromatographic separation was performed on an Agilent ZORBAX Eclipse Plus C18 Rapid Resolution HT column (2.1 × 100 mm, 1.8 µm) maintained at 40 °C. For sample preparation, 1000 µg of dried plant extract was dissolved in 250 µL of methanol, vortexed thoroughly, and sonicated for 15 minutes. The solution was then diluted with 250 µL of distilled water, centrifuged for 15 minutes, and the resulting clear supernatant was filtered before being transferred into a glass vial for analysis. The mobile phases consisted of (A) 0.1% formic acid in distilled water and (B) 0.1% formic acid in acetonitrile, optimized for positive ionization mode. The mobile phases consisted of (A) 0.1% ammonium formate in distilled water and (B) acetonitrile, optimized for negative ionization mode. The gradient elution program was as follows: 0.00–18.00 min, 5–95% B; 18.00–23.00 min, 95% B; and 23.01 min, 5% B. The total run time was 30 minutes, with a 2-minute re-equilibration before each injection. The injection volume was 2 µL, and the mobile phase flow rate was set at 0.25 mL/min. The mass spectrometer was operated under the following conditions: gas temperature 325 °C, gas flow 11 L/min, and nebulizer pressure 35 psi. Data acquisition and analysis were performed using Agilent MassHunter Qualitative Analysis software (version B.05.00; Agilent Technologies, Santa Clara, CA, USA) (Begum *et al*., 2025a).

Molecular docking analysis

The compounds identified through Q-ToF-LCMS analysis of the *T. macrophylla* leaf's methanol extract were further investigated using an *in silico* molecular docking approach against two target proteins. The chemical structures of both the standard drugs (Dabrafenib, Ormeloxifene) and the compounds were retrieved from the PubChem database (https://pubchem.ncbi.nlm.nih.gov/). For the docking study, the human estrogen receptor alpha ligand-binding domain (PDB ID: 3ERT) (Shiau et al., 1998) and the BRaf Kinase mutant (PDB ID: 3OG7) (Bollag *et al*., 2020) (Fig. 3) were selected as target proteins and obtained from the Protein Data Bank (http://www.rcsb.org). Protein structures were prepared by removing water molecules and native ligands, followed by the addition of polar hydrogens. For 3ERT, redocking of the native ligand (OHT600) was performed using grid points (X, Y, Z) set to 28, 28, and 28, respectively, with coordinate grid points (X, Y, Z) at 30.01, -1.913, and 24.206, ensuring a root-mean-square deviation (RMSD) less than 2. For 3OG7, redocking of the native ligand (vemurafenib) was performed by setting grid points (X, Y, Z) to 46, 16, and 36, respectively, and coordinate grid points (X, Y, Z) at 2.643, -2.28, and -19.403, ensuring that the RMSD was less than 2. Molecular docking analyses were conducted using Discovery Studio, Autodock Tools 1.5.7, and AutoDock Vina (Trott & Olson, 2010). The docking results were subsequently examined through both 2D and 3D visualizations to provide detailed insights into the binding interactions (Begum *et al*., 2025b; Ahmed *et al*., 2026).

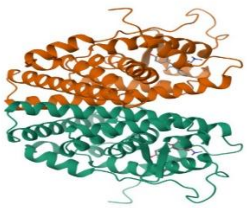

(A)

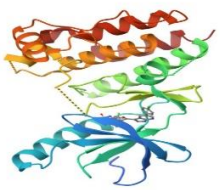

(B)

Fig. 3: 3D structures of two selected proteins: PDB ID 3ERT (A) and PDB ID 3OG7 (B) along with their respective native ligands.

Physicochemical and pharmacokinetics properties

The study of physicochemical and pharmacokinetic properties is considered extremely important for forecasting a drug's behaviour within the human body, augmenting its therapeutic efficacy and ensuring its safety. Accordingly, the bioactive constituents of the methanol extract, identified via LC/MS-QTOF analysis, were assessed for their potential impact on drug absorption and distribution. Particular emphasis was placed on solubility, lipophilicity, and molecular size, as these parameters are key determinants of pharmacokinetic performance. In addition, these properties govern how a drug is metabolized by the liver and other organs, as well as the rate at which it is eliminated from the body (http://www.swissadme.ch/index.php, https://biosig.lab.uq.edu.au/pkcsm/prediction) (Begum *et al*. 2025c).

Results and discussion

% yield and Q-ToF LCMS analysis

The methanol extract (yield: 9.29%) revealed a number of compounds identified through Q-ToF LCMS analysis. The chromatograms obtained from the Q-ToF LCMS analysis are presented in Fig. 4, while the chemical structures of selected compounds are illustrated in Fig. 5. The identified compounds were analysed through LC-MS/MS in positive and negative ionization modes to further confirm their tentative structures, as shown in Fig. A1. Table 1 contains the tentatively identified compounds from *T. macrophylla* leaf methanol extract by LCMS Q-ToF investigation along with the mass error and annotation level.

Error mass calculation is a cornerstone of analytical accuracy in liquid chromatography mass spectrometry (LC-MS/MS). It quantifies the deviation between the measured and theoretical mass-to-charge ratio (m/z) of an analyte, serving as a critical metric for both qualitative identification and quantitative analysis. Accurate error mass determination is essential for confident compound assignment, regulatory compliance, and reliable clinical or environmental measurements. It normalizes the mass difference to the theoretical mass, allowing comparison across analytes of different sizes. High-resolution mass spectrometers (QTOF) routinely achieve error mass values <5 ppm, enabling confident assignment of chemical formulae and structural elucidation (Kellmann et al., 2019; Smith et al., 2018). The error mass is calculated by the formula: Error (ppm) = [(Measured m/z - Theoretical m/z) / Theoretical m/z] × 10^6

In addition, compound annotation in LC-MS/MS is a critical step in metabolomics and exposomics studies, enabling the identification and characterization of chemical entities. The annotation process is often categorized into Level 1 and Level 2 based on the confidence in compound identification. Level 2 annotation involves probable identification based on spectral similarity, database matching, or predictive models, without direct confirmation by standards. It relies on computational tools, spectral libraries, and cheminformatics approaches (Ljoncheva et al., 2020; Shen et al., 2022; Zheng et al., 2022).

Among the identified compounds, the majority belong to the flavonoid class, several of which have already been reported in the literature for their anticancer potential. Apigenin, for instance, has been shown to exert anticancer effects by modulating a wide range of cell signalling pathways, including tumor suppressor genes, angiogenesis, apoptosis, cell cycle regulation, inflammation, PI3K/AKT, NF-κB, MAPK/ERK and STAT3 pathways. Consequently, apigenin has demonstrated efficacy against multiple cancer types, particularly breast and skin cancers (Rahmani et al., 2022). Based on these findings, the identified compound apigenin 7-(2''-*E*-*p*-coumaroylglucoside may also possess significant anticancer properties. Similarly, 3,3′,4′,7-tetrahydroxyflavone, commonly known as fisetin, has been reported to inhibit cancer cell proliferation and invasion stages, suppress cell growth, and induce programmed cell death (Imran et al., 2020). Therefore, other identified flavonoids such as epifisetinidol-4alpha-ol, 5,7,4'-trihydroxyflavanone 7-sulfate, and 7,8,4'-trihydroxyflavanone may likewise exhibit potent anticancer activities.

Table 1: Tentatively identified phytoconstituents from *T. macrophylla* leaf methanol extract by LCMS Q-ToF investigation.

SI NO	Putative Compound (Molecular formula)/ Ionization mode	Obtained RT (min)	Score (%)	Obtained *m/z* ($M+H^+$/$M-H^+$)	Exact mass (Da)	Mass Error (ppm)	Annotation Level	Predicted LCMS/MS Fragmentation	References
1.	Apigenin 7-(2''-*E*-*p*-coumaroylglucoside ($C_{30}H_{26}O_{12}$)/ negative ionization	2.484	73.33	577.1344	578.1424	-1.2	Level 2	$[M-H]^-$ at *m/z* 577.1344 $[M-H-CO_2]^-$ at *m/z* 530.3031 [M-p-coumaroyl]$^-$ at *m/z* 451.1018 [Apigenin-glucoside-H]$^-$ at *m/z* 407.0747 [Apigenin-H]$^-$ at *m/z* 381.1033 Retro-Diels-Alder (RDA) cleavage of apigenin at *m/z* 289.0694 p-Coumaric acid fragment ($C_9H_7O_3^-$) at *m/z* 161.0167 Fragment of *p*-coumaric acid ($C_7H_5O_2^-$) at *m/z* 125.0250	Hagazy & Mulata, 2016
2.	Epifisetinidol-4alpha-ol ($C_{15}H_{14}O_6$)/ negative ionization	3.683	85.67	289.0718	290.0790 1.0073	0.3	Level 2	$[M-H]^-$ at *m/z* 289.057 $[M-H-H_2O]^-$at *m/z* 273.0791 $[M-H-CO-H_2O]^-$ at *m/z* 256.0234 Ring cleavage fragment at *m/z* 245.0792 RDA cleavage at *m/z* 227.0804 A-ring fragment ($C_9H_7O_4^-$) at *m/z* 179.0269 B-ring fragment ($C_8H_5O_4^-$) at *m/z* 165.0135	Jiang & Gates, 2024
3.	Urolithin A-3-O-glucuronide ($C_{19}H_{16}O_{10}$)/ negative ionization	5.411	88.39	403.0654	404.0744	-4.2	Level 2	$[M-H]^-$ at *m/z* 403.0654 $[M-H-C_6H_8O_6]^-$at *m/z* 273.0791 $[M-H-C_6H_8O_6-H_2O]^-$at *m/z* 256.0234 [Urolithin A-H]$^-$ at *m/z* 227.0804 A-ring fragment ($C_9H_7O_4^-$) at *m/z* 179.0269 B-ring fragment ($C_8H_5O_4^-$) at *m/z* 165.013	Kang et al., 2023

4.	Isovitexin (C_{21} H_{20} O_{10})/ negative ionization	6.861	98.38	431.0989	432.1057	1.2	Level 2	$[M-H]^-$ at *m/z* 431.0989 $[M-H-CO_2]^-$ at *m/z* 397.202 $[M-H-CO_2-H_2O]^-$ at *m/z* 373.8612 $[M-H-C_6H_{10}O_5]^-$ at *m/z* 289.0658	Yan et al., 2013
5.	Epicatechin monogallate (C_{22} H_{18} O_{10})/negative ionization	7.05	80.58	441.0824	442.0900	0.5	Level 2	[M-H]- at m/z 441.0824 [M-H-Galloyl]- at *m/z* 289.0638 (Epicatechin) Gallic acid derived fragment at *m/z* 169.0135 RDA fragment of epicatechin at *m/z* 271.0591 [M-H-B ring ($C_6H_5O_2$)]- at m/z 332.0047 ($C_{16}H_{11}O_8$)-	Ousji & Sleno, 2022
6.	6-Hydroxyluteolin 5-rhamnoside (C_{21} H_{20} O_{11})/ negative ionization	7.638	94.32	447.0934	448.1006	0.2	Level 2	$[M-H]^-$at *m/z* 447.0934 $[M-H-H_2O]^-$ at *m/z* 425.1015 $[M-H-CO_2]^-$ at *m/z* 393.0806 $[M-H-CO_2-H_2O]^-$ at *m/z* 369.1049 Aglycone-side fragment at *m/z* 289.0725	Hagazy & Mulata, 2016; Es-Safi et al., 2005
7.	5,7,4'-Trihydroxyflavanone 7-sulfate (C_{15} H_{12} O_8 S)/ negative ionization	8.198	98.75	351.0181	352.0253	0.3	Level 2	$[M-H]^-$ at *m/z* 351.0181 $[M-H-36]^-$ (e.g., -H_2O-O) at *m/z* 315.0468 $[M-H-51]^-$ (e.g.,-CO-H_2O) at *m/z* 300.0242 Aglycone $[A-H]^-$ via -SO_3 at *m/z* 271.0599	Hagazy & Mulata, 2016
8.	7,8,4'-Trihydroxyflavanone (C_{15} H_{12} O_5)/positive ionization	10.831	85.18	273.0758	272.0687	-0.7	Level 2	$[M+H]^+$ at *m/z* 273.0758 $[M+H-H_2O]^+$ at *m/z* 255.0687 A-ring cation (resorcinol-type) at *m/z* 153.0183 B-ring cation (catechol/guaiacol-type) at *m/z* 147.0430	Hagazy & Mulata, 2016
9.	4,2',3',4'-Tetrahydroxychalcone (C_{15} H_{12} O_5)/ negative ionization	11.007	98.13	271.0617	272.0685	1.8	Level 2	$[M-H]^-$ at *m/z* 271.0617 $[M-H-CO]^-$ at *m/z* 258.9215 $[M-H-CO-H]^-$ at *m/z* 245.0583 RDA cleavage product (A/B-ring derived) at *m/z* 223.1367 Catechol-type B-ring fragment -CO/-CO_2 at *m/z* 198.9710 A-ring	Hagazy & Mulata, 2016

								phenoxide (resorcinol/phloroglucinol) at *m/z* 192.9952	
10.	Epigallocatechin 3-O-caffeate (C_{24} H_{20} O_{10})/positive ionization	11.916	78.26	469.1124	468.1057 1.0073	-1.3	Level 2	$[M+H]^+$ at *m/z* 469.1124 $[M+H\text{-caffeic acid}]^+$ at *m/z* 345.1001 Caffeic-derived aryl cation (-H_2O/-CO variants) at *m/z* 234.0974 Caffeic acid-related tropylium/aryl cation at *m/z* 162.0756	Ousji & Sleno, 2022

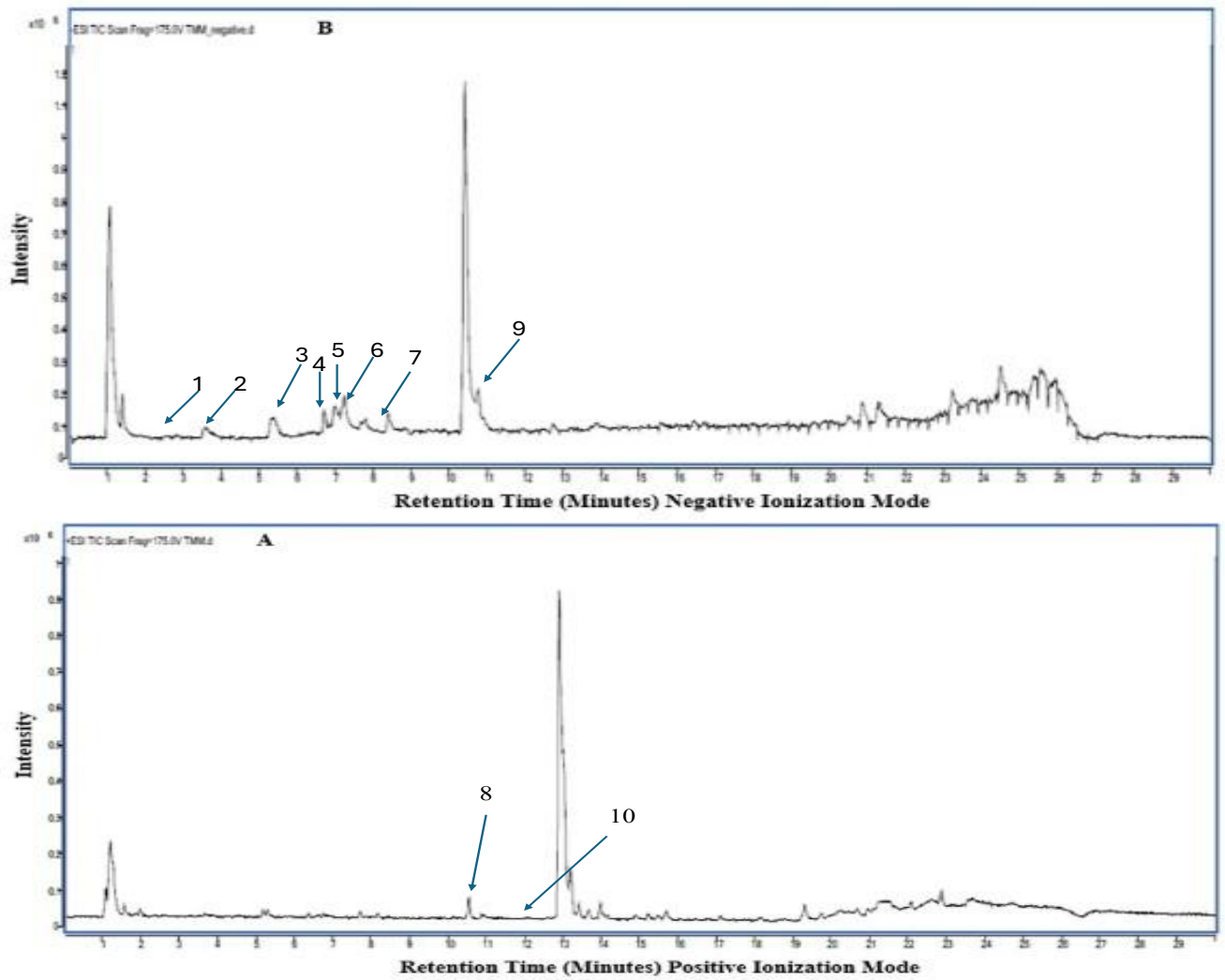

Fig. 4: Total Ion Chromatograms from Q-ToF LCMS analysis of *Tetracera macrophylla* leaf methanol extract, obtained in both positive (A) and negative (B) ionization modes.

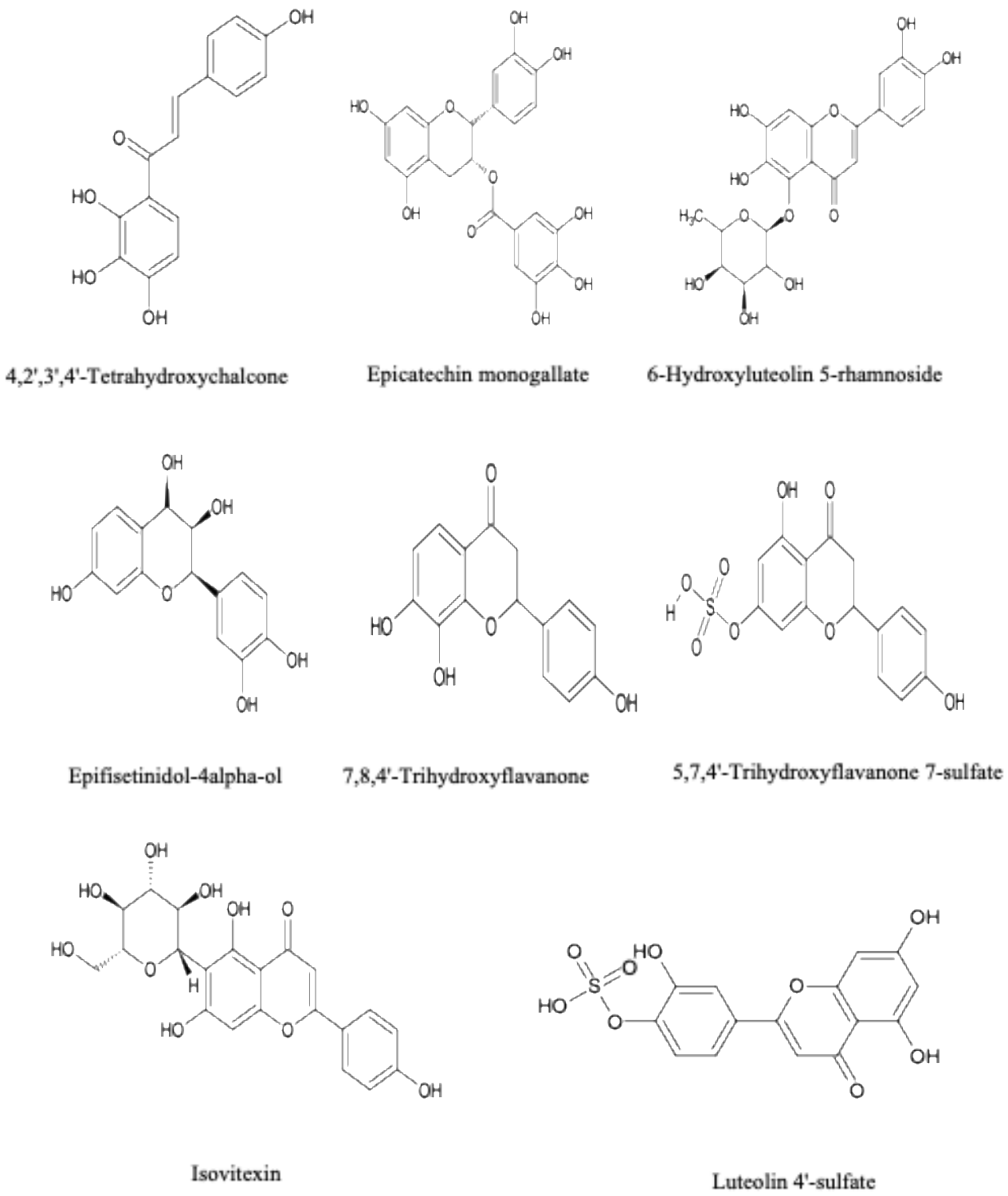

Fig. 5: Chemical structures of some compounds obtained through Q-ToF LCMS analysis of *T. macrophylla* leaf methanol extract.

The anticancer properties of luteolin have been extensively investigated across multiple cancer types and are associated with its ability to inhibit tumour growth by targeting key cellular processes, including apoptosis, angiogenesis, migration, and cell cycle progression (Çetinkaya & Baran, 2023). This highlights the potential anticancer activity of the identified compound 6-hydroxyluteolin 5-rhamnoside. Similarly, (−)-epicatechin exhibits strong antioxidant by interacting with and neutralizing reactive oxygen species within cells. In addition, it modulates cell signalling pathways, such as the MAP kinase pathway, which plays a critical role in cell proliferation. The use of (-)-epicatechin has shown promise both as a preventive agent and as an adjunct to chemotherapy and radiation therapy, enhancing treatment outcomes (Shay et al., 2015). Furthermore, (-)-epicatechin has been demonstrated to induce apoptosis in breast cancer cells, regardless of receptor status (Pereyra-Vergara et al., 2020). Based on these findings, the identified compounds epicatechin monogallate, and epigallocatechin 3-O-caffeate from the methanol extract of *T. macrophylla* leaves may possess potent anticancer properties.

Molecular docking against anticancer proteins

Molecular docking of the compounds identified through Q-ToF LCMS analysis of the methanol extract of *T. macrophylla* leaves was performed against two cancer-related target proteins: the human estrogen receptor alpha (breast cancer, PDB ID: 3ERT) and BRaf kinase mutant (melanoma, PDB ID: 3OG7). For 3ERT, the native ligand and the standard drug (ormeloxifene) exhibited binding energies of -9.9 and -8.6 kcal/mol, respectively. In comparison, several of the ten tested compounds demonstrated strong binding affinities, including apigenin 7-(2''-*E*-*p*-coumaroylglucoside (-8.8 kcal/mol), epicatechin monogallate (-8.7 kcal/mol), 7,8,4'-trihydroxyflavanone (-8.5 kcal/mol), epigallocatechin 3-O-caffeate (-8.3 kcal/mol), 5,7,4'-trihydroxyflavanone 7-sulfate (-8.2 kcal/mol), and Urolithin A-3-O-glucuronide (-8.2 kcal/mol) (Table 2, Fig. 6). The binding interactions of the remaining six compounds with 3ERT are provided in the appendix (Fig. A2).

The native ligand (OHT600) formed a hydrogen bond with the GLU 353 of the protein 3ERT, while additional interactions were observed with LEU 346, MET 421, LEU 525, ALA 350, and LEU 387. For apigenin 7-(2''-E-p-coumaroylglucoside), residues LEU 536, TRP 383, LEU 346, ALA 350, and LEU 525 contributed to various interactions. In case of epicatechin monogallate, hydrogen bonding was established with CYS 530 and ALA 350. Additionally, GLU 353 and TRP 383 were involved in hydrogen bond formation with 7,8,4'-trihydroxyflavanone. Furthermore, GLU 353, ARG 394 and LEU 387 were involved to establish hydrogen bond in Urolithin A-3-O-glucuronide. The standard drug showed diverse interactions with amino acids, including CYS 530, LEU 384, LEU 525, TRP 383, MET 522, LEU 536, and VAL 533. Overall, the tested compounds demonstrated comparable amino acid involvement to that observed with both the native ligand and the standard drug.

For the protein 3OG7, the native ligand and the standard drug exhibited binding energies of -11.1 and -9.0 kcal/mol, respectively. Among the ten tested compounds, apigenin 7-(2''-*E*-*p*-coumaroylglucoside (-10.3 kcal/mol), 6-hydroxyluteolin 5-rhamnoside (-9.9 kcal/mol), epigallocatechin 3-O-caffeate (-9.9 kcal/mol), isovitexin (-9.3 kcal/mol), epicatechin monogallate (-9.2 kcal/mol), 5,7,4'-trihydroxyflavanone 7-sulfate (-9.1 kcal/mol), and 7,8,4'-trihydroxyflavanone (-9.1 kcal/mol) demonstrated the strongest binding affinities (Table 3, Fig. 7). The binding interactions of the remaining six compounds with 3OG7 are provided in the appendix (Fig. A3).

The native ligand (vemurafenib) formed hydrogen bond with the GLN 530, GLY 596, and PHE 595 of the protein 3ERT. Additional interactions were observed with ILE 463, TRP 531, CYS 532, LEU 505, LYS 483, PHE 583, LEU 514, ALA 481, and PHE 595. In the case of apigenin 7-(2''-E-p-coumaroylglucoside, GLY 534, and CYS 532 were involved in distinct interactions. 6-hydroxyluteolin 5-rhamnoside exhibited hydrogen bonding with SER 465, ILE 463, ASN 580, ASN 581, and GLN 530. For epigallocatechin 3-O-caffeate, ILE 527 was responsible for hydrogen bond formation. The standard drug showed hydrogen bonds with amino acids namely ASP 594, and ASN 590, while additional interactions were observed with the PHE 468, LYS 578, SER 465, ASN 580, ASP 594, ASN 581, VAL 471, TRP 531, and PHE 583. Overall, the tested compounds demonstrated comparable amino acid involvement to that of both the native ligand and the standard drug.

Table 2: The profiling of compounds of methanol extract of *T. macrophylla* leaves interaction with the 3ERT protein.

Compounds	Ligand binding energy (kcal/mol)	Binding Interactions	
		Different bond interactions other than H bond with bond distance (Å)	H bond interactions with bond distance (Å)
4,2',3',4'-Tetrahydroxychalcone	-7.8	LEU 346: 4.00; LEU 525: 5.28; TRP 383: 4.44; ALA 350: 5.05 & 5.24	THR 347: 2.70
5,7,4'-Trihydroxyflavanone 7-sulfate	-8.2	LEU 525: 4.59; MET 343: 5.89; ALA 350: 4.46 & 5.09; LEU 346: 4.85	ASP 351: 2.81
6-Hydroxyluteolin 5-rhamnoside	-8.0	LEU 525: 5.36; LEU 354: 5.13; TRP 383: 4.36: ALA 350: 5.25; LEU 536: 5.20 & 4.75	MET 522: 2.84
7,8,4'-Trihydroxyflavanone	-8.5	LEU 391: 4.92; LEU 387: 5.23 & 4.39; LEU 384: 5.10; ALA 350: 4.10 & 4.89; LEU 346: 4.55; LEU 525: 4.87; MET 343: 4.87	GLU353: 2.04
Apigenin 7-(2''-*E*-*p*-coumaroylglucoside	-8.8	LEU 536: 4.37; TRP 383: 5.35; LEU 346: 4.49; ALA 350: 3.87; LEU 525: 4.70; 4.73 & 5.04	-
Epicatechin monogallate	-8.7	ALA 350: 5.02; TRP 383: 4.73; LEU 536: 4.01; LYS 529: 3.58	CYS 530: 2.88; ALA 350: 3.38
Epifisetinidol-4alpha-ol	-7.8	LEU 346: 5.30; ALA 350" 4.62; LEU 387: 4.59; LEU 525: 4.88; MET 421: 5.33	GLU 535: 2.66
Epigallocatechin 3-O-caffeate	-8.3	LEU 354: 5.22; ALA 350: 5.36; TRP 383: 4.40; LEU 536: 5.13; LEU 525: 5.08; TYR 526: 5.03	MET 522: 2.22; LEU 536: 2.67; ASP 351: 2.08
Isovitexin	-8.1	LEU 536: 5.39; 5.24 & 5.39; TRP 383: 4.39; LEU 354: 5.25; ALA 350: 5.09	CYS 530: 2.11
Urolithin A-3-O-glucuronide	-8.2	MET 343: 5.17; THR 347: 3.68; ALA 350: 4.02 & 3.90; LEU 525: 5.10; 4.78 & 4.29	LEU 387: 3.09; GLU 353: 2.30; ARG 394: 2.82
Native Ligand: OHT600	-9.9	LEU 346: 4.98 & 4.94; MET 421: 4.77 & 5.24; LEU 525: 4.88 & 4.78; ALA 350: 4.12; LEU 387: 5.01	GLU 353: 2.50
Standard drug: Ormeloxifene	-8.6	CYS 530: 5.50; LEU 384: 5.26; LEU 525: 4.30; 4.22 & 5.41; TRP 383: 5.69 & 5.45; MET 522; 4.61; LEU 536: 5.22; VAL 533: 5.42	-

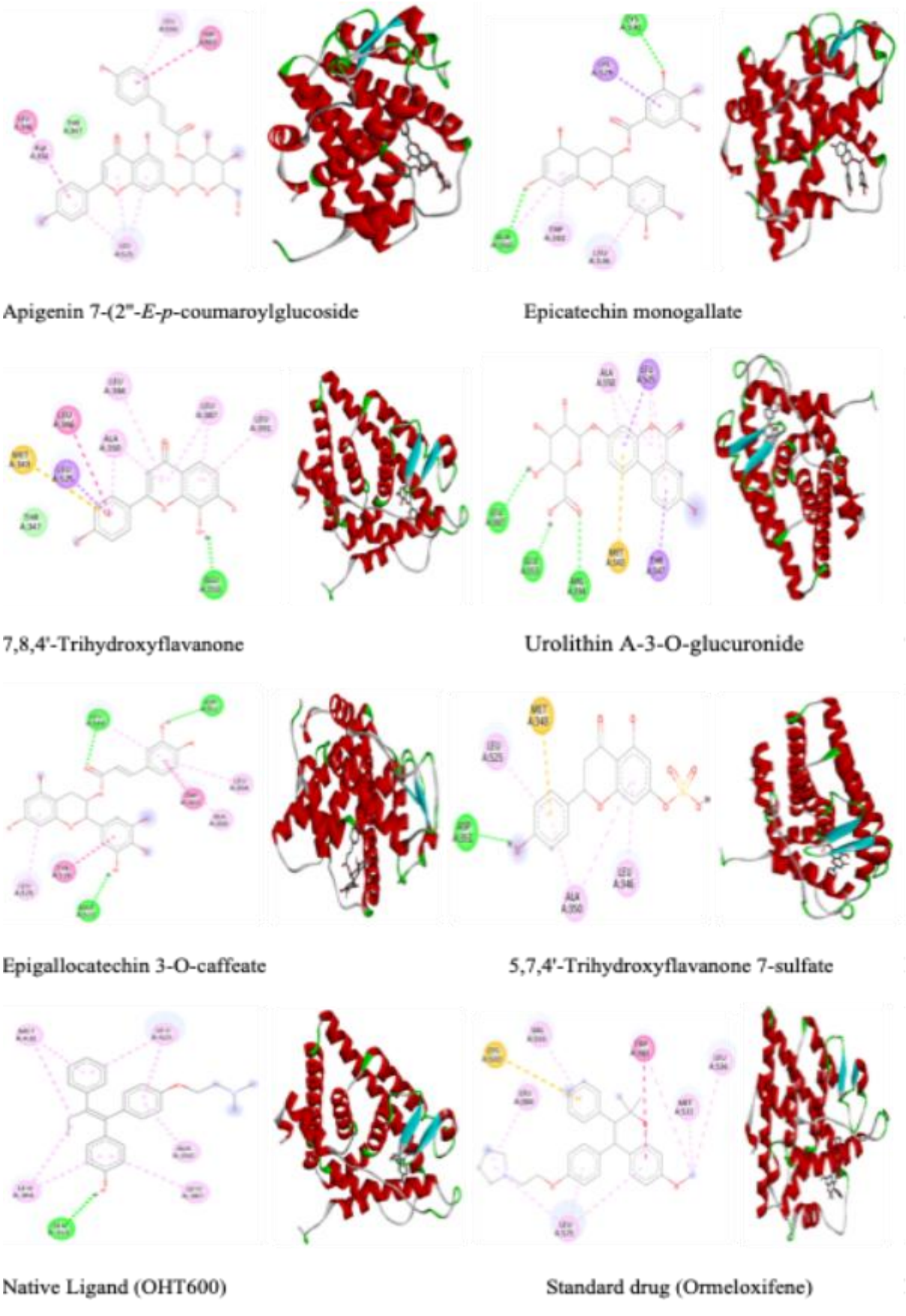

Fig. 6: Binding interactions of apigenin 7-(2''-*E*-*p*-coumaroylglucoside, epicatechin monogallate, 7,8,4'-trihydroxyflavanone, Urolithin A-3-O-glucuronide, epigallocatechin 3-O-caffeate, and 5,7,4'-trihydroxyflavanone 7-sulfate along with the native ligand and standard with the 3ERT protein.

Table 3: The profiling of compounds of methanol extract of *T. macrophylla* leaves interaction with the 3OG7 protein.

Compounds	Ligand binding energy (kcal/mol)	Binding Interactions	
		Different bond interactions other than H bond with bond distance (Å)	H bond interactions with bond distance (Å)
4,2',3',4'-Tetrahydroxychalcone	-8.3	CYS 532: 5.77; TRP 531: 4.92 & 3.77; PHE 583: 4.68; LYS 483: 3.97; VAL 471: 5.35	ASP 594: 1.93; CYS 532: 3.02
5,7,4'-Trihydroxyflavanone 7-sulfate	-9.1	LEU 514; 5.45; LYS 483: 4.14; CYS 532: 5.68; PHE 583: 3.96; VAL 471: 5.36	ASP 594: 2.03; PHE 595: 2.40; GLY 596; 2.09
6-Hydroxyluteolin 5-rhamnoside	-9.9	CYS 532: 4.91; ALA 481: 4.30; PHE 583: 5.13 & 4.38; VAL 471: 4.65, 3.67 & 5.49	SER 465; 2.94; ILE 463: 3.06; ASN 580: 1.70 & 2.53; ASN 581: 2.27 & 2.10; GLN 530: 1.92
7,8,4'-Trihydroxyflavanone	-9.1	CYS 532: 5.26; PHE 583: 4.03; ALA 481: 4.94 & 4.33; LEU 514: 5.42; LYS 483: 5.14 & 3.99; VAL 471: 5.47 & 4.69	ASP 594: 2.36
Apigenin 7-(2''-*E*-*p*-coumaroylglucoside	-10.3	LEU 514: 5.03; LYS 483: 5.22; ALA 481: 4.46; ILE 463: 5.33; VAL 471: 5.47 & 5.24; TRP 531: 5.85 & 5.26	GLY 534: 2.59; CYS 532: 1.93
Epicatechin monogallate	-9.2	LEU 514: 5.44; ALA 481: 4.47; PHE 583: 4.47; VAL 471: 4.74 & 5.17	SER 536: 2.23; CYS 532: 2.56; THR 529: 2.75
Epifisetinidol-4alpha-ol	-8.5	LYS 483: 3.85; PHE 583: 3.91; CYS 532: 5.49; VAL 471: 5.49	ILE 527: 2.55; THR 529: 2.04
Epigallocatechin 3-O-caffeate	-9.9	LYS 483: 3.70; VAL 471: 5.06; PHE 583: 4.65 & 5.45; CYS 532: 5.50	ILE 527: 2.93
Isovitexin	-9.3	TRP 531: 5.41; VAL 471: 3.90 & 5.13; ALA 481; 5.49; ILE 463: 5.27	ASP 594; 1.80
Urolithin A-3-O-glucuronide	-9.1	GLY 466: 3.76; ALA 481: 445; CYS 532: 5.25; TRP 531: 5.42; VAL 471: 4.36, 4.13 & 5.13	GLN 530: 2.64; SER 465: 2.10; ASP 594: 2.23; LYS 578: 3.08
Native Ligand: Vemurafenib	-11.1	ILE 463: 4.66; TRP 531: 5.93; CYS 532: 5.00; LEU 505: 4.06; LYS 483: 4.10; PHE 583: 4.75; LEU 514: 4.83; ALA 481: 3.79; PHE 595: 4.59	GLN 530: 2.24; GLY 596: 2.21; PHE 595: 2.68
Standard drug: Dabrafenib	-9.0	PHE 468: 5.09; LYS 578: 4.27; SER 465: 3.27; ASN 580: 3.29; ASP 594: 3.13; ASN 581: 3.57; VAL 471: 4.70 & 5.07; TRP 531: 5.02; PHE 583: 4.50 & 3.53	ASP 594: 2.60; ASN 590: 1.83

Physicochemical and Pharmacokinetic parameters

The drug likeness properties of the ten identified compounds were performed by assessing their physicochemical and ADMET properties, which are include in Table 4. A total eight compounds, such as, isovitexin, epigallocatechin 3-O-caffeate, 5,7,4'-trihydroxyflavanone 7-sulfate, 7,8,4'-trihydroxyflavanone, 4,2',3',4'-tetrahydroxychalcone, urolithin A-3-O-glucuronide, epifisetinidol-4alpha-ol, and epicatechin monogallate exhibited drug likeness by obeying Lipinski's Rule of Five (Ananda et al., 2025). However, urolithin A-3-O-glucuronide, and epifisetinidol-4alpha-ol showed either hepatotoxicity or AMES toxicity, whereas the remaining drug like six compounds were free from any detectable toxicities. Intestinal absorption, a critical pharmacokinetic parameter, was moderate for most of these compounds, ranging from 47.642% (apigenin 7-(2''-*E*-*p*-coumaroylglucoside) to 68.365% (4,2',3',4'-tetrahydroxychalcone). The only exception was 7,8,4'-trihydroxyflavanone, which showed a higher intestinal absorption rate of 94.25%. Taken together, and considering literature evidence, molecular docking results, as well as physicochemical and pharmacokinetic parameters assessments, six of the ten compounds identified exhibited strong potential as lead candidates for the development of novel anticancer drugs targeting breast cancer and melanoma.

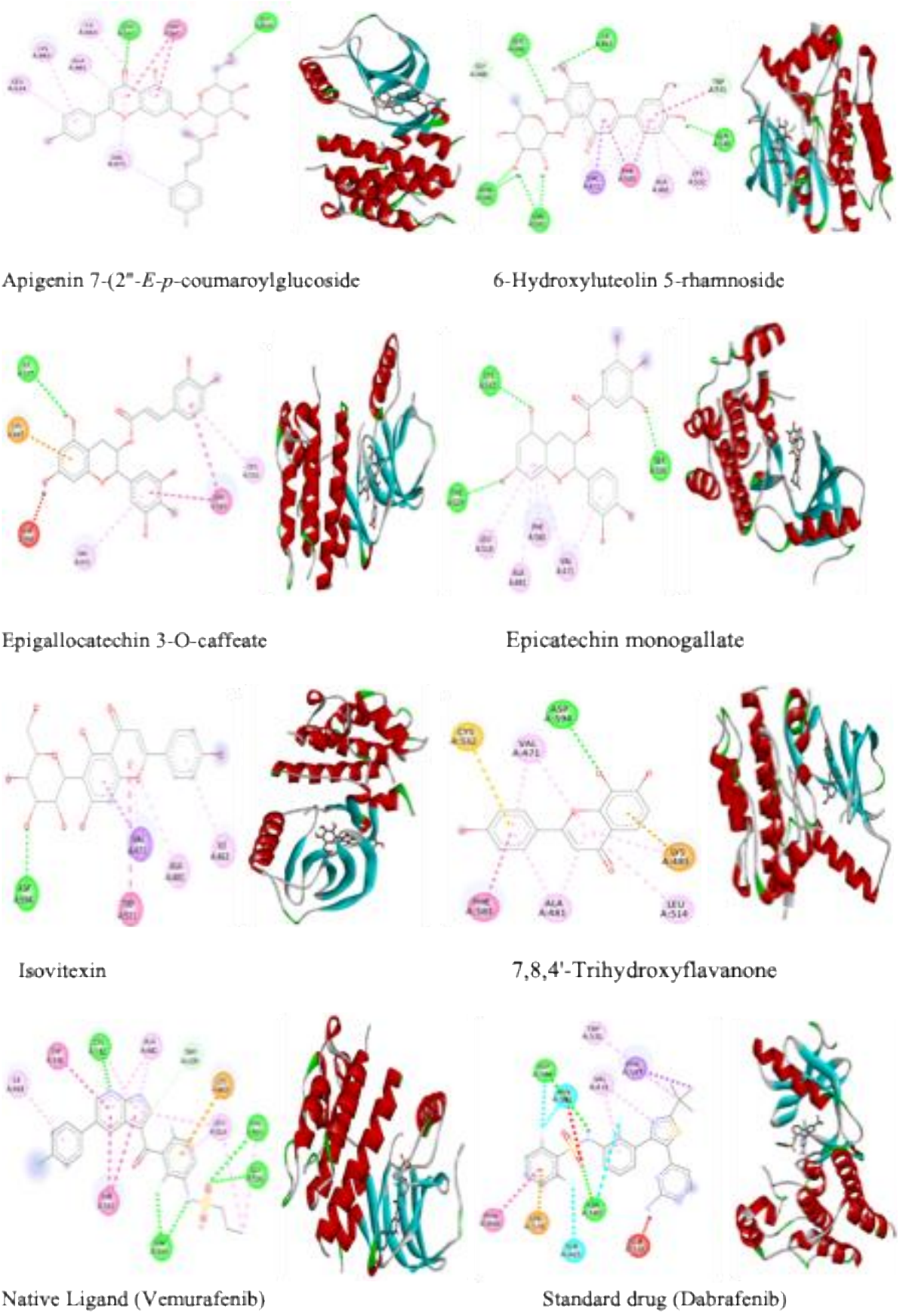

Fig. 7: Binding interactions of apigenin 7-(2''-*E*-*p*-coumaroylglucoside, 6-hydroxyluteolin 5-rhamnoside, epigallocatechin 3-O-caffeate, epicatechin monogallate, isovitexin and 7,8,4'-trihydroxyflavanone along with the native ligand and standard drug with the 3OG7 protein.

1

2

3

Table 4: Physicochemical and ADMET profiles of tentative compounds identified in *T. macrophylla* methanol leaf extract.

Compound (MW)	Characteristics									
	Physicochemical					Pharmacokinetic				
	H-Ac	H-Do	Log P	DL	NVL	CL	IA	AT	ROAT	HT
Isovitexin (432.38)	10	7	-2.02	Yes	1	0.557	64.729	No	2.558	No
Epigallocatechin 3-O-caffeate (468.41)	10	7	0.40	Yes	1	-0.096	51.082	No	2.558	No
Urolithin A-3-O-glucuronide (404.32)	10	5	-0.47	Yes	0	0.695	31.563	No	0.644	Yes
6-Hydroxyluteolin 5-rhamnoside (448.38)	11	7	-1.84	No	2	0.57	53.78	No	2.556	No
Apigenin 7-(2''-*E*-*p*-coumaroylglucoside (578.52)	12	6	-0.56	No	3	0.193	47.642	No	2.615	No
Epifisetinidol-4alpha-ol (290.27)	6	5	-0.02	Yes	0	0.003	65.555	Yes	2.45	No
5,7,4'-Trihydroxyflavanone 7-sulfate (352.32)	8	3	0.19	Yes	0	0.094	55.498	No	2.446	No
7,8,4'-Trihydroxyflavanone (270.24)	5	3	0.52	Yes	0	-0.073	94.25	No	2.45	No
4,2',3',4'-Tetrahydroxychalcone (272.25)	5	4	1.02	Yes	0	-0.063	68.365	No	1.948	No
Epicatechin monogallate (442.37)	10	7	0.05	Yes	1	-0.073	56.152	No	2.693	No

Note: H-Ac - Number of Hydrogen Acceptors; H-Do - Number of Hydrogen Donors; Log P - Predicted Octanol/Water Partition Coefficient; DL - Drug-Likeness; NVL - Number of Lipinski's Rule Violations; CL - Clearance (log mL/kg/day); IA - Intestinal Absorption; AT - Ames Toxicity; ROAT - Oral Rat Acute Toxicity (mol/kg); HT - Hepatotoxicity; MW - Molecular Weight.

Conclusion

The concept of extracts and individual compounds differs in several important aspects. Extracts represent a complex mixture of diverse classes of compounds, and their biological activity often reflects the combined effects of these phytoconstituents, including possible agonistic or antagonistic interactions. Therefore, when an extract exhibits potent activity in biological assays, the observed effect may be the net result of multiple compound interactions rather than the action of a single molecule. To determine the precise bioactivity, isolation and characterization of the active compounds from the extract is essential. The present study is the first to investigate the anticancer potential of compounds derived from *T. macrophylla* extract. By identifying six lead compounds, it provides a strong foundation for future research aimed at developing novel anticancer drugs targeting melanoma and breast cancer.

Authors contributions

Conceptualization, T.B. and Q.U.A.; methodology, T.B.; software, S.A.A.S., M.S.R. and Z.I.; validation, Q.U.A., K.R. and Z.I.; formal analysis, T.B.; investigation, T.B. and M.A.H.A.R.; resources, Q.U.A., S.A.A.S., and M.S.R.; data curation, T.B.; writing-original draft preparation, T.B.; writing—review and editing, Q.U.A., M.H.A., A.H.U. and A.K.; visualization, K.R. and Z.I.; supervision, Q.U.A.; project administration, Q.U.A.; funding acquisition, Q.U.A. All authors have read and agreed to the published version of the manuscript.

Acknowledgements

This work was partially supported by CRIGS UKM-IIUM-UiTM-UPM Research Collaboration Grant 2024 (C-RIGS24-017-0023), Research Management Centre, International Islamic University Malaysia (IIUM), Malaysia.

Conflict of interest

The authors declare no conflicts of interest.

Declaration of generative AI and AI-assisted technologies in the writing process

No AI (e.g. ChatGPT, Gemini and others) was used to improve readability and language during the preparation of this work.

References

Ahmed, Q. U., Ab Rahim, M. A. H., Arzmi, M. H., Uddin, A. H., Ali Shah, S. A., Rofiee, M. S., Parveen, H., Mukhtar, S., Faridi, U., Rosedi, M. H. M., Sarian, M. N., & Begum, T. (2026). Antimicrobial and antioxidant activities of *Tetracera macrophylla* Hook. f. & Thomson leaf extracts: insights from Q-ToF-LCMS, pharmacokinetics and molecular docking approach. Natural Product Research, 1-15. https://doi.org/10.1080/14786419.2026.2654646

Ananda, Z. K, Begum, T., Ahda, M., Rofiee, M. S., Shah, S. A. A., Salleh, M. Z. Almutairi, B. O., Azmi, S. N. H., Sah, P, Wardani, A. K., Khatib, A., Abbas, S. A., Mia, M. A. R., & Ahmed, Q. U. (2025). Comparative evaluation of phytochemical screening, *in vitro* antioxidant & alpha-glucosidase inhibitory properties of *Ceiba pentandra* & *Basella rubra* leaf extracts: Identification of active principles by Q-TOFLCMS, ADMET prediction & molecular docking approach. Journal of King Saud University–Science, 37(1), 162024. https://doi.org/10.25259/JKSUS_16_2024.

Begum, T., Ahmed, Q. U., Arzmi, M. H., Shah, S. A. A., Rofiee, et al. (2025c). Targeting Diabetes Pathways: An *in silico* Study of Bioactive Compounds from *Mitragyna speciosa* Leaf Extract. International Journal of Allied Health Sciences, 9(SUPP3). IIUM Press

Begum, T., Ahmed, Q. U., Arzmi, M. H., Uddin, A. H., Khatib, A., et al. (2025a). Phytochemical screening and evaluation of in vitro antioxidant, antibacterial and antibiofilm activities of *Mitragyna speciosa* leaf extract. Malaysian Journal of Chemistry, 27(5), 80-94. https://doi.org/10.55373/mjchem.v27i5.80

Begum, T., Arzmi, M. H., Uddin, A. H, Rofiee, M. S., Shah, S. A. A., et al. (2025b). Unveiling comparative bioactivities of Kratom leaf extracts obtained via maceration and ultrasonic techniques: Antioxidant, antimicrobial, and antibiofilm effects with molecular docking of Q-ToF-LCMS identified compounds and ADMET prediction. Journal of King Saud University–Science, 37(10). https://doi.org/0.25259/JKSUS_1185_2025

Bray, F., Laversanne, M., Sung, H., Ferlay, J., Siegel, R. L., Soerjomataram, I., & Jemal, A. (2024). Global cancer statistics 2022: GLOBOCAN estimates of incidence and mortality worldwide for 36 cancers in 185 countries. CA: a cancer journal for clinicians, 74(3), 229-263. https://doi.org/10.3322/caac.21834

Castellani, G., Buccarelli, M., Arasi, M. B., Rossi, S., Pisanu, M. E., et al.. (2023). BRAF mutations in melanoma: biological aspects, therapeutic implications, and circulating biomarkers. Cancers, 15(16), 4026. https://doi.org/10.3390/cancers15164026

Çetinkaya, M., & Baran, Y. (2023). Therapeutic potential of luteolin on cancer. Vaccines, 11(3), 554. https://doi.org/10.3390/vaccines11030554

Es-Safi, N. E., Kerhoas, L., Einhorn, J., & Ducrot, P. H. (2005). Application of ESI/MS, CID/MS and tandem MS/MS to the fragmentation study of eriodictyol 7-O-glucosyl-(1→ 2)-glucoside and luteolin 7-O-glucosyl-(1→ 2)-glucoside. International Journal of Mass Spectrometry, 247(1-3), 93-100. https://doi.org/10.1016/j.ijms.2005.10.002

Hagazy, K., & Mulata, H. N. (2016). Structural characterization of flavonoids using mass spectrometry. Research & Reviews: A Journal of Pharmacology, 6, 1-19. STM Journals.

Imran, M., Saeed, F., Gilani, S. A., Shariati, M. A., Imran, A., Afzaal, M., Atif, M., Tufail, T., Anjum, F. M. (2021). Fisetin: An anticancer perspective. Food science & nutrition, 9(1), 3-16. https://doi.org/10.1002/fsn3.1872

Jiang, C., & Gates, P. J. (2024). Systematic characterisation of the fragmentation of flavonoids using high-resolution accurate mass electrospray tandem mass spectrometry. Molecules, 29(22), 5246. https://doi.org/10.3390/molecules29225246

Kang, M. J., Suh, J. H., Guarneiri, L. L., Cooper, J. A., & Paton, C. M. (2023). LC–MS analysis of urolithin-related metabolites in human plasma reveals glucuronide conjugates as the primary species after 4-weeks of pecan consumption. Journal of Food Bioactives, 21. https://doi.org/10.31665/JFB.2023.18336

Kellmann, M., Muenster, H., Zomer, P., & Mol, H. (2009). Full scan MS in comprehensive qualitative and quantitative residue analysis in food and feed matrices: how much resolving power is required?. Journal of the American Society for Mass

Spectrometry, 20(8), 1464-1476. https://doi.org/10.1016/j.jasms.2009.05.010

Ladeska, V., Elya, B., Hanafi, M., & Kusmardi. (2023). Pharmacognostic evaluation and antioxidant capacity of *Tetracera macrophylla* Hook. F. & Thoms twigs. Journal of Pharmacy & Pharmacognosy Research, 11(3), 523–536. https://doi.org/10.56499/jppres23.1613_11.3.523

Ljoncheva, M., Stepišnik, T., Džeroski, S., & Kosjek, T. (2020). Cheminformatics in MS-based environmental exposomics: Current achievements and future directions. Trends in environmental analytical chemistry, 28, e00099. https://doi.org/10.1016/j.teac.2020.e00099

Mazlun, M. H., Sabran, S. F., Abdullah, Z., Parumasivam, T. (2021). A comparative study of antituberculosis activities of *Tetracera macrophylla* Wall. Ex Hook. f. & thoms. stem fractions using different chromatographic stationary phases. IOP Conference Series: Earth and Environmental Science, 736(1). https://doi.org/10.1088/1755-1315/736/1/012036

Ousji, O., & Sleno, L. (2022). Structural elucidation of novel stable and reactive metabolites of green tea catechins and alkyl gallates by LC-MS/MS. Antioxidants, 11(9), 1635. https://doi.org/10.3390/antiox11091635

Pereyra-Vergara, F., Olivares-Corichi, I. M., Perez-Ruiz, A. G., Luna-Arias, J. P., & García-Sánchez, J. R. (2020). Apoptosis induced by (−)-epicatechin in human breast cancer cells is mediated by reactive oxygen species. Molecules, 25(5), 1020. https://doi.org/10.3390/molecules25051020

Rahmani, A. H., Alsahli, M. A., Almatroudi, A., Almogbel, M. A., Khan, A. A., Anwar, S., & Almatroodi, S. A. (2022). The potential role of apigenin in cancer prevention and treatment. Molecules, 27(18), 6051. https://doi.org/10.3390/molecules27186051

Sahayarayan, J. J., Rajan, K. S., Vidhyavathi, R., Nachiappan, M., Prabhu, D., Alfarraj, S., Arokiyaraj, S., & Daniel, A. N. (2021). *In-silico* protein-ligand docking studies against the estrogen protein of breast cancer using pharmacophore based virtual screening approaches. Saudi Journal of Biological Sciences, 28(1), 400-407. https://doi.org/10.1016/j.sjbs.2020.10.023

Shay, J., Elbaz, H. A., Lee, I., Zielske, S. P., Malek, M. H., & Hüttemann, M. (2015). Molecular mechanisms and therapeutic effects of (−)-epicatechin and other polyphenols in cancer, inflammation, diabetes, and neurodegeneration. Oxidative medicine and cellular longevity, 2015(1), 181260. https://doi.org/10.1155/2015/181260

Shen, X., Wu, S., Liang, L., Chen, S., Contrepois, K., Zhu, Z. J., & Snyder, M. (2022). metID: an R package for automatable compound annotation for LC− MS-based data. Bioinformatics, 38(2), 568-569. https://doi.org/10.1093/bioinformatics/btab583

Shiau, A. K., Barstad, D., Loria, P. M., Cheng, L., Kushner, P. J., Agard, D. A., & Greene, G. L. (1998). The structural basis of estrogen receptor/coactivator recognition and the antagonism of this interaction by tamoxifen. Cell, 95(7), 927-937. https://doi.org/10.1016/s0092-8674(00)81717-1

Smith, D. F., Podgorski, D. C., Rodgers, R. P., Blakney, G. T., & Hendrickson, C. L. (2018). 21 tesla FT-ICR mass spectrometer for ultrahigh-resolution analysis of complex organic mixtures. Analytical chemistry, 90(3), 2041-2047. https://doi.org/10.1021/acs.analchem.7b04159

Yan, C., Liu, H., & Lin, L. (2013). Simultaneous determination of vitexin and isovitexin in rat plasma after oral administration of Santalum album L. leaves extract by liquid chromatography tandem mass spectrometry. Biomedical Chromatography, 27(2), 228-232. https://doi.org/10.1002/bmc.2780

Zheng, F., You, L., Qin, W., Ouyang, R., Lv, W., Guo, L., Lu, X., Li., E., Zhao, X., & Xu, G. (2022). MetEx: a targeted extraction strategy for improving the coverage and accuracy of metabolite annotation in liquid chromatography–high-resolution mass spectrometry data. Analytical chemistry, 94(24), 8561-8569. https://doi.org/10.1021/acs.analchem.1c04783

World Health Organization. Health topics: cancer. Available at: https://www.who.int/health-topics/cancer#tab=tab_1.

Appendix (Supplementary Material)

Putative Compound	Molecular formula	Observed RT (min)	Observed *m/z*	Score	Ionization mode
Apigenin 7-(2"-*E*-*p*-coumaroylglucoside	$C_{30}H_{26}O_{12}$	2.484	577.1344	73.33	-ve
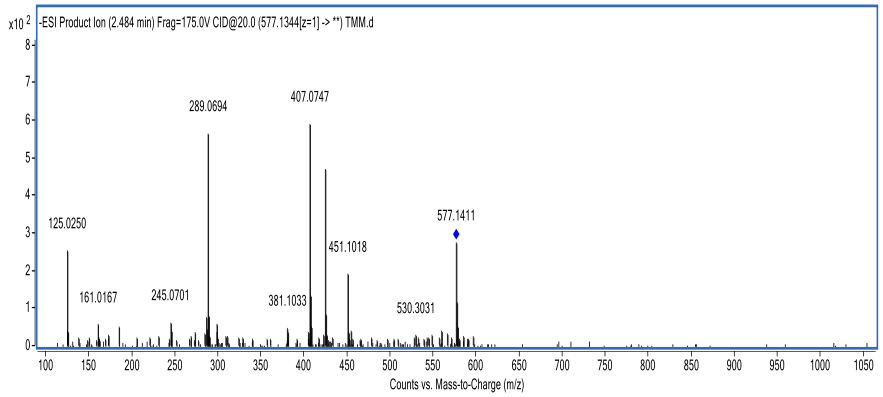	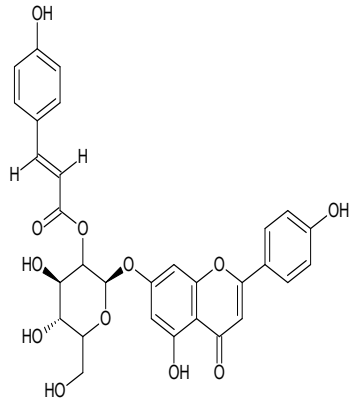				
Epifisetinidol-4alpha-ol	$C_{15}H_{14}O_6$	3.683	289.0718	85.67	-ve
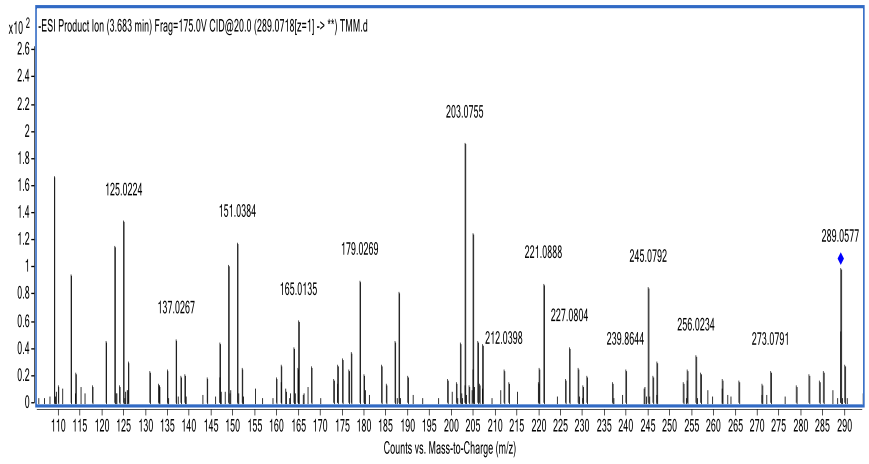	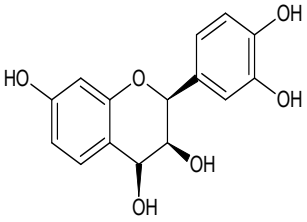				
Urolithin A-3-O-glucuronide	$C_{19}H_{16}O_{10}$	5.411	403.0654	88.39	-ve
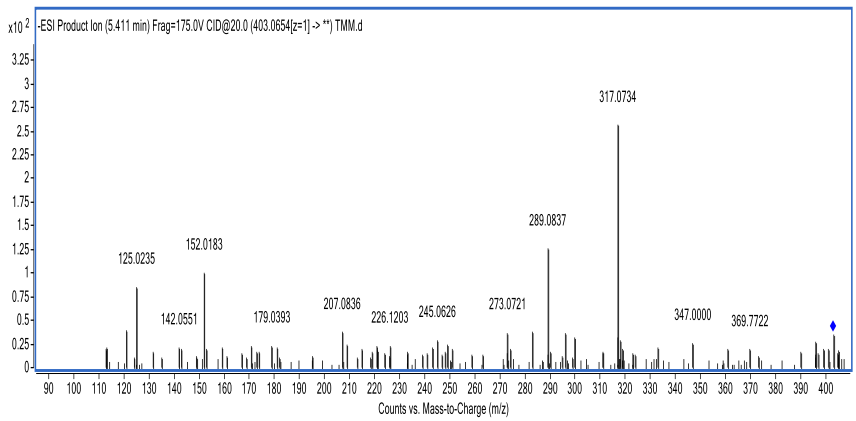	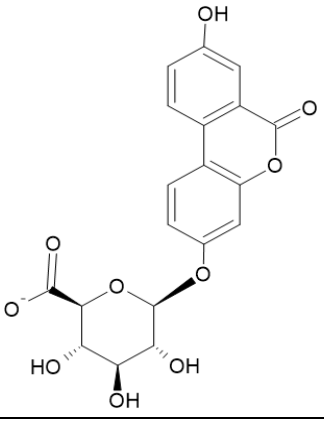				

Isovitexin	$C_{21}H_{20}O_{10}$	6.861	431.0989	98.38	-ve
Epicatechin monogallate	$C_{22}H_{18}O_{10}$	7.05	441.0824	80.58	-ve
6-Hydroxyluteolin 5-rhamnoside	$C_{21}H_{20}O_{11}$	7.638	447.0934	94.32	-ve

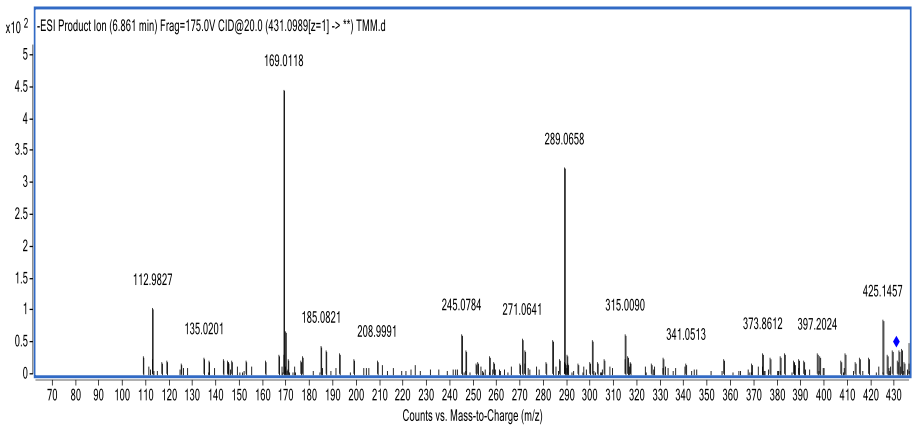

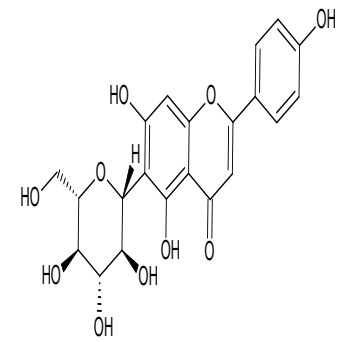

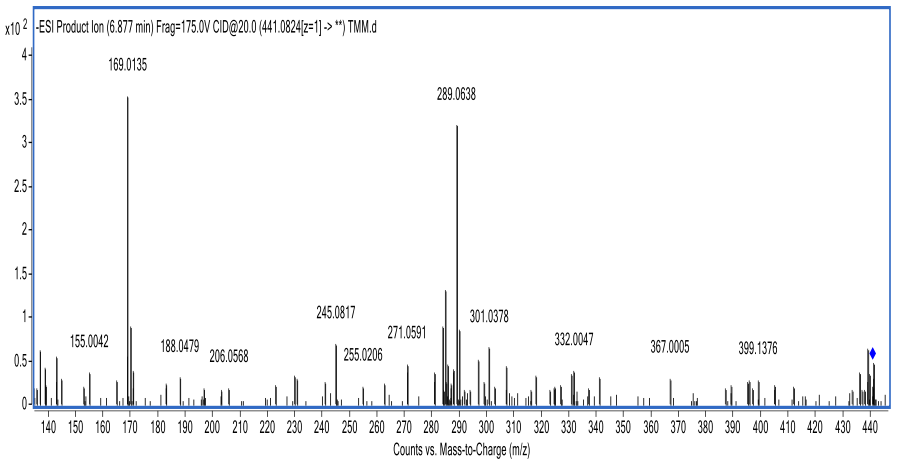

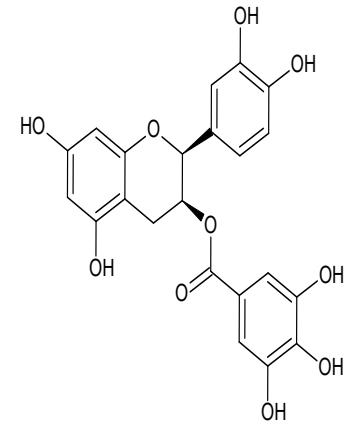

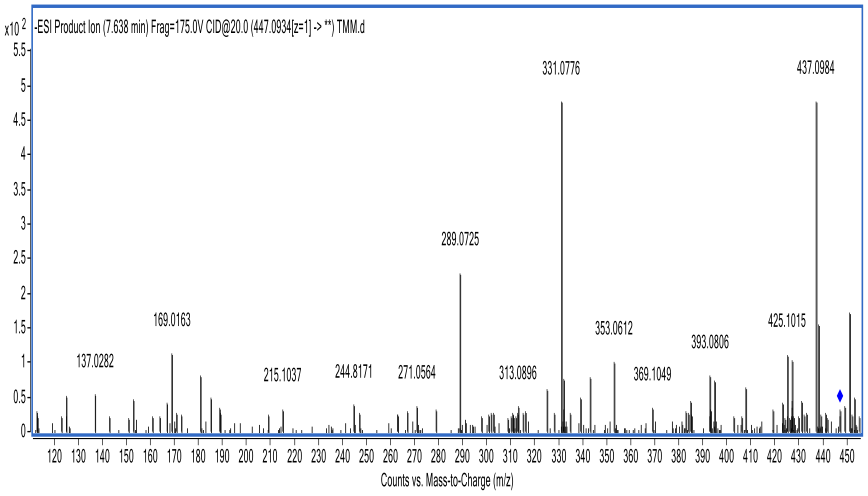

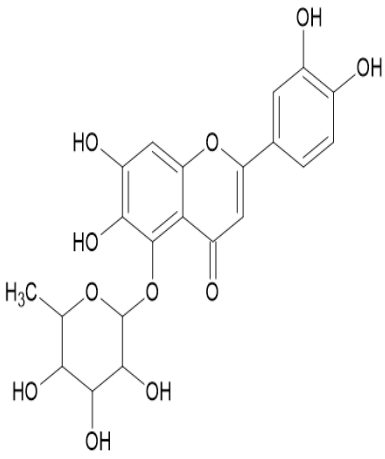

5,7,4'-Trihydroxyflavanone 7-sulfate	$C_{15}H_{12}O_8S$	8.198	351.0181	98.75	-ve

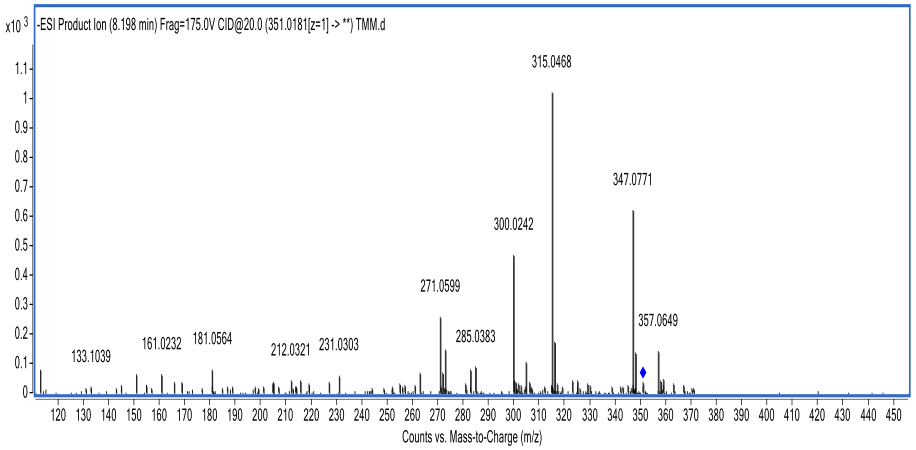

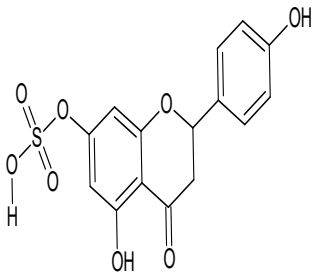

4,2',3',4'-Tetrahydroxychalcone	$C_{15}H_{12}O_5$	11.007	271.0617	98.13	-ve

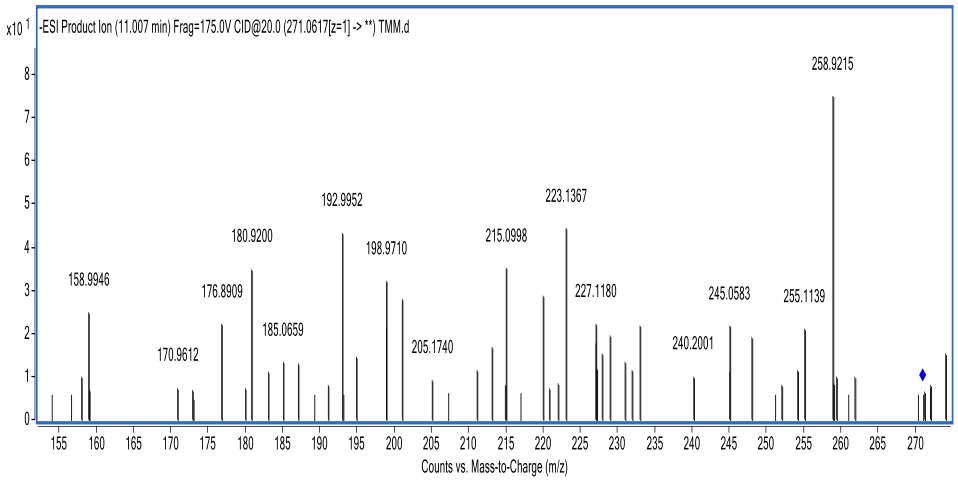

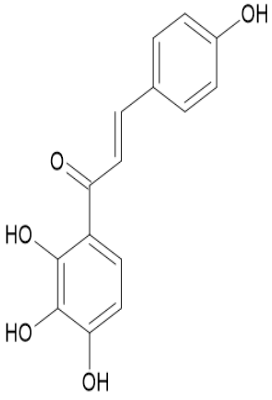

7,8,4'-Trihydroxyflavanone	$C_{15}H_{12}O_5$	10.831	273.0758	85.18	+ve

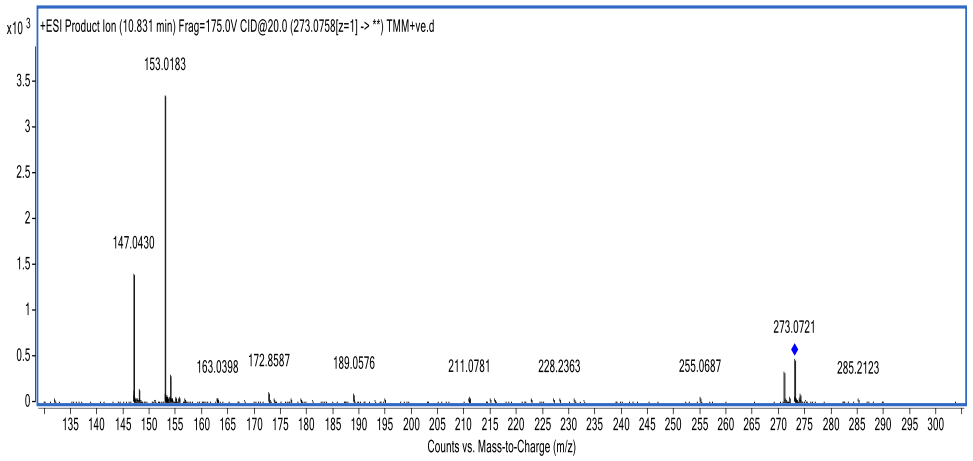

Epigallocatechin 3-O-caffeate	C_{24} H_{20} O_{10}	11.916	469.1124	78.26	+ve

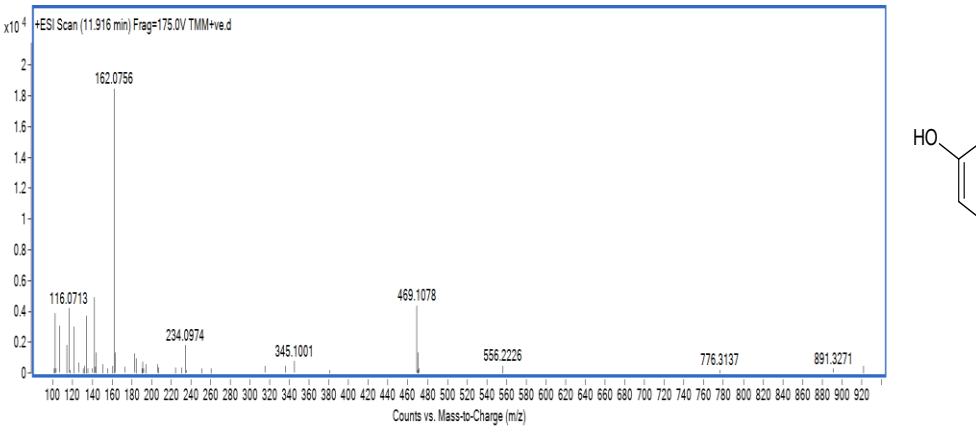

Fig. A1: QTOF LC–MS chromatograms of the methanolic leaf extract of *T. macrophylla*, displaying MS/MS spectra for each detected m/z value under both positive and negative ionization modes.

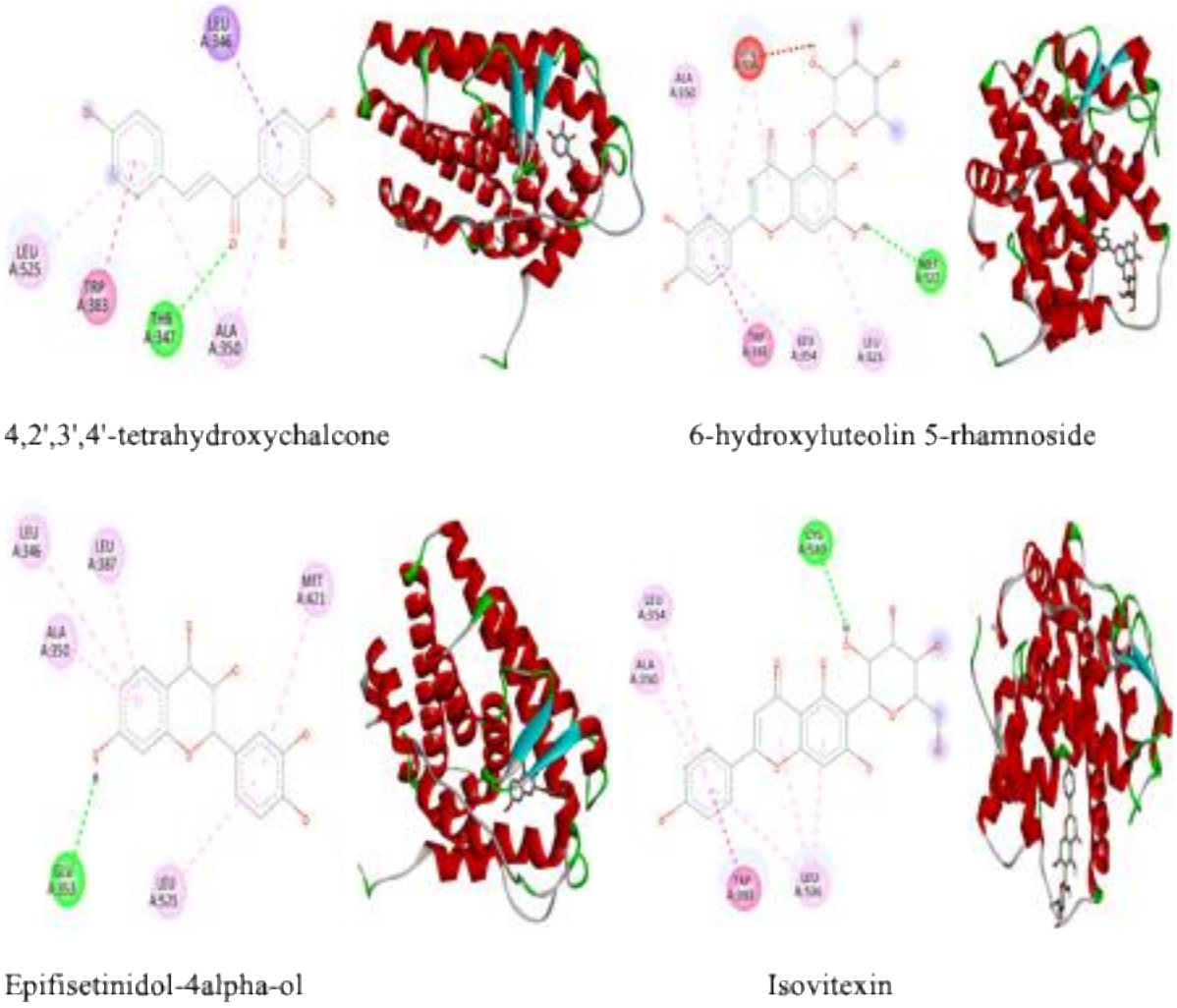

Fig. A2: Binding interactions of 4,2',3',4'-tetrahydroxychalcone, 6-hydroxyluteolin 5-rhamnoside, epifisetinidol-4alpha-ol, and isovitexin with the 3ERT protein.

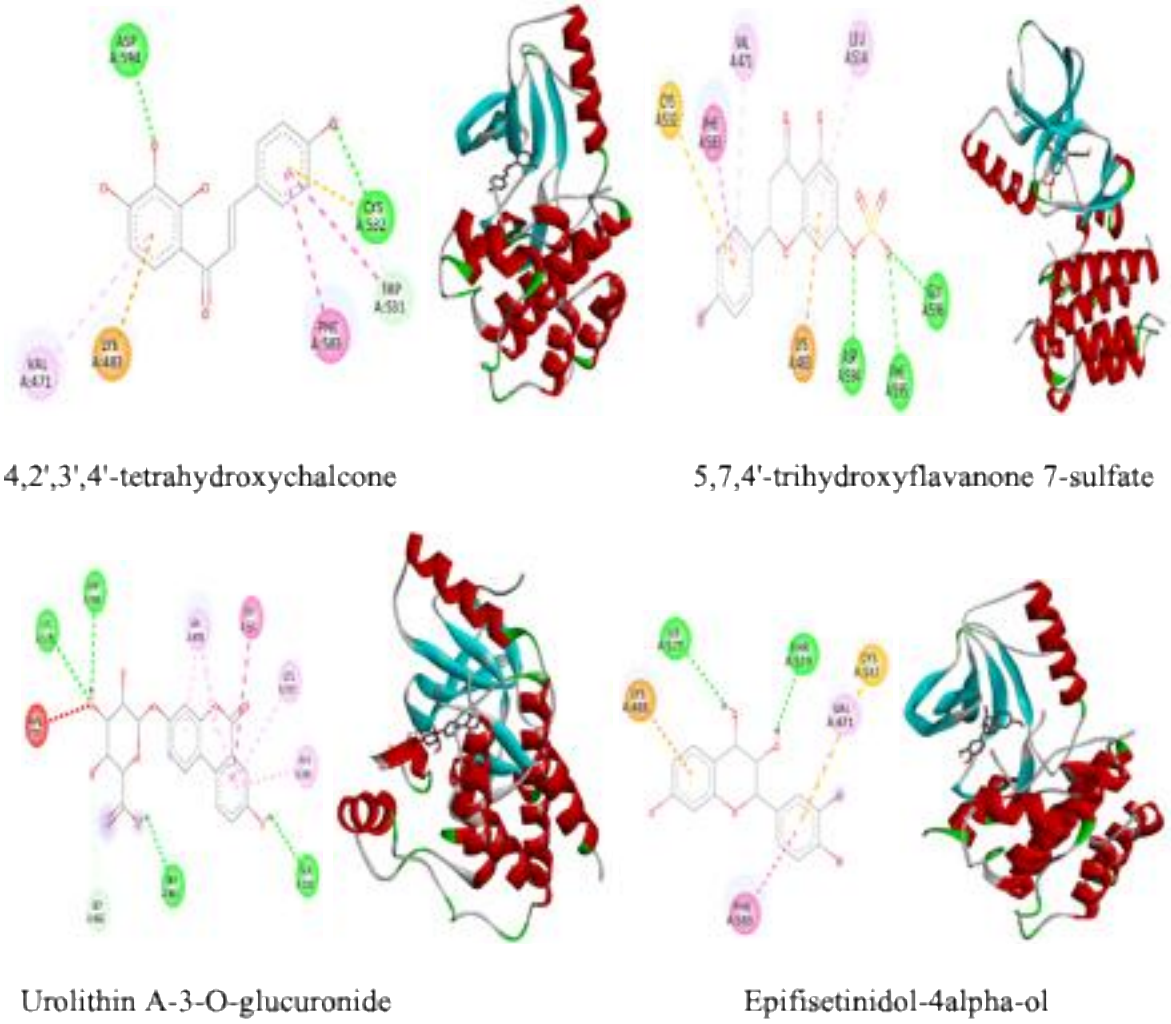

Fig. A3: Binding interactions of 4,2',3',4'-tetrahydroxychalcone, 5,7,4'-trihydroxyflavanone 7-sulfate, urolithin A-3-O-glucuronide, and epifisetinidol-4alpha-ol with the 3OG7 protein.